

A CORRELATION FOR SINGLE PHASE TURBULENT MIXING IN SQUARE ROD ARRAYS UNDER HIGHLY TURBULENT CONDITIONS

HAE-YONG JEONG*, KWI-SEOK HA, YOUNG-MIN KWON, WON-PYO CHANG and YONG-BUM LEE

Korea Atomic Energy Research Institute

150 Deokjin-dong, Yuseong-gu, Daejeon 305-353, Korea

*Corresponding author. E-mail : hyjeong@kaeri.re.kr

Received January 11, 2006

Accepted for Publication October 24, 2006

The existing experimental data related to the turbulent mixing factor in rod arrays is examined and a new definition of the turbulent mixing factor is introduced to take into account the turbulent mixing of fluids with various Prandtl numbers. The new definition of the mixing factor is based on the eddy diffusivity of energy. With this definition of the mixing factor, it was found that the geometrical parameter, δ_{ij}/D_h , correlates the turbulent mixing data better than S/d , which has been used frequently in existing correlations. Based on the experimental data for a highly turbulent condition in square rod arrays, a correlation describing turbulent mixing dependent on the parameter δ_{ij}/D_h has been developed. The correlation is insensitive to the Re number and it takes into account the effect of the turbulent Prandtl number. The proposed correlation predicts a reasonable mixing even at a lower S/d ratio.

KEYWORDS : Turbulent Mixing, Subchannel Analysis, Mixing Factor, Gap Stanton Number, Mixing Coefficient

1. INTRODUCTION

For the safe and reliable operation of a reactor system, it is very important to predict the detailed flow and temperature distributions in the thermal-hydraulic design of a reactor core. Accurate flow and temperature distributions are usually calculated with a subchannel approach, in which the temperature, pressure and velocity in a subchannel are averaged, and one representative thermal-hydraulic condition specifies the state of the subchannel. To obtain the flow and temperature distributions with a subchannel analysis code, conservations of the mass, momentum, and energy in a subchannel are modelled and solved. Therefore, it is necessary to model the inter-subchannel mixing phenomenon due to the cross flow between the adjacent subchannels as accurately as possible in order to enhance the predictability of the subchannel analysis code [1,2].

When a single-phase flow exists in the subchannels, the mixing of the mass, energy and momentum between the subchannels consists of two parts: a forced mixing and a natural mixing. The natural mixing also consists of a diversion flow and a turbulent mixing. The diversion flow mixing is mainly caused by a pressure gradient due to flow obstacles such as spacers or due to differences in density. The turbulent mixing, caused by the eddy motion of the fluid across the gap between the subchannels, enhances

the exchange of the momentum and the energy through the gap with no net transport of the mass.

If there is no diversion flow or forced mixing flow, the energy transport across a gap between the subchannels per unit length in rod bundles is equivalent to

$$q_{ij} = k \left(1 + \text{Pr} \frac{\varepsilon_H}{\nu} \right) S_{ij} \left(\frac{\partial T}{\partial n} \right)_s, \quad (1)$$

where k is the thermal conductivity of the fluid, ν is the kinematic viscosity, S_{ij} is the gap width between subchannels i and j . In Fig. 1, the geometry of a square rod array is depicted. The dominant turbulent mixing occurs parallel to the wall across a gap between two rods, i.e., in the direction of the coordinate z in the figure.

The equation above indicates that the energy transfer occurs due to heat conduction through the coolant itself and due to the turbulent eddy motion of the fluid. Under the typical operating conditions of a pressurized water reactor (PWR), the second term in the first bracket of Eq. (1) is of the order of 10^3 . Therefore, the level of heat transfer by conduction is negligible in the design of a PWR. In contrast, the order of the same quantity for a liquid metal-cooled reactor (LMR) is approximately $10^{-1} \sim 10^0$, which implies that both heat conduction and turbulent mixing

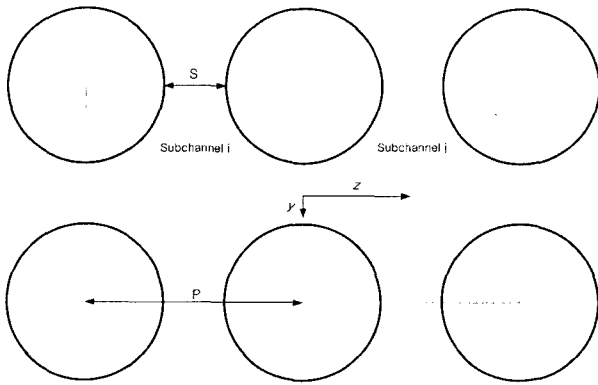


Fig. 1. Coordinates and Subchannel Geometry for a Square Rod Array

play important roles in the thermal-hydraulics of an LMR. It should be noted that the modeling of turbulent mixing is very important for the thermal hydraulics of both a PWR and an LMR.

The turbulent mixing model in a subchannel code determines the turbulent mixing flow rate w' and the turbulent momentum factor f_T . The turbulent momentum factor is identical to the turbulent Prandtl number. The turbulent mixing flow rate from subchannel i to j per unit length is defined with the effective mean fluctuating velocity w_{eff} , as follows:

$$w'_{ij} = \rho_i w_{eff} S_{ij}, \tag{2}$$

where ρ_i is the density of the fluid in subchannel i .

2. PREVIOUS WORKS

Many experimental results with rod bundles have obtained much higher turbulent mixing rates than those predicted by conventional turbulent diffusion theories for a simple geometry. These experimental results imply that the eddy diffusivity of energy, ϵ_M , for rod bundles is much higher than that obtained in a circular tube. Initially, several researchers attempted to explain this high turbulent mixing rate in terms of the effect of the secondary flow formed in the subchannels. However, direct measurements of turbulent structures in rod arrays [3] have suggested that the main cause of the high mixing rate in compact rod bundles is due to a cyclic and periodic flow pulsation, which is sometimes referred to as the anisotropic turbulent motion. Therefore, researchers have concentrated their efforts on developing a useful correlation by taking into account the anisotropic component of turbulence in rod bundles. As a result of these efforts, several correlations have been developed with different definitions of the mixing parameters.

The most general form of the existing correlations on

turbulent mixing in rod bundles has been developed with a definition of the turbulent mixing coefficient β , defined by the ratio of the effective mean mixing velocity to the axial velocity. The definition is:

$$\beta = \frac{w_{eff}}{u}. \tag{3}$$

This mixing coefficient is essentially the same as the gap Stanton number, St_g . This definition of a mixing coefficient was used in the correlations suggested by Row and Angle [4], Castellana [5], Seale [6], Cheng and Todreas [7]. The turbulent mixing coefficient is normally determined from the thermal mixing test under single-phase conditions. With this definition of a turbulent mixing coefficient, the turbulent mixing flow rate from channels i to j is

$$w'_{ij} = \beta S_{ij} \bar{G}_{ij}, \tag{4}$$

where \bar{G}_{ij} is the average axial mass flux flowing along subchannels i and j . Some researchers, such as Ramm [8], and Rogers and Tahir [9] have suggested correlations with the mixing flow rate divided by the dynamic viscosity, which are easily converted to a correlation with the mixing coefficient β per the relationship of Eq. (4).

The other type of mixing factor, Y , was first suggested by Ingesson and Hedberg [10]. Other researchers such as Rehme [3] and Moller [11] have also adopted the same definition of a mixing factor in their studies. The turbulent mixing factor, Y , is defined in the following equation for a heat transfer through a gap per unit length by

$$q_{ij} = \rho c_p \bar{\epsilon}_M S_{ij} Y \frac{T_i - T_j}{\delta_{ij}}, \tag{5}$$

where $\bar{\epsilon}_M$ is the reference eddy viscosity obtained in a circular tube and δ_{ij} is the centroid distance between subchannels i and j . In addition, c_p is the specific heat of the fluid, T_i and T_j are the fluid temperatures in subchannels i and j , respectively. The same heat transport is also described with an effective mean mixing velocity, as follows:

$$q_{ij} = \rho c_p w_{eff} S_{ij} (T_i - T_j) \tag{6}$$

A comparison between Eqs. (5) and (6) yields a more direct expression of Y , as follows:

$$Y = \frac{w_{eff} \delta_{ij}}{\bar{\epsilon}_M}. \tag{7}$$

Therefore, the turbulent mixing through a gap between two neighboring subchannels per unit length is described as follows:

$$w'_{ij} = \frac{\rho S_{ij} \bar{\epsilon}_M}{\delta_{ij}} Y. \tag{8}$$

Through intensive studies of the structure of the turbulence in the subchannels of rod bundles, Rehme [3] concluded that the natural mixing between the subchannels mainly results from the periodic flow pulsations, and that the secondary flow motion does not contribute significantly to the mixing process. He derived the following correlation based on a large amount of experimental data from investigation results ranging from the early 1960's to 1990:

$$Y = \frac{0.7}{\left(\frac{S_{ij}}{d} \right)}, \tag{9}$$

where d is the diameter of a rod.

Although a considerable scattering of the data was found in the derivation of the correlation, the mixing factor developed by Rehme [3] is simple and can be effectively used for any gap geometry, as the structure of turbulence due to periodic flow pulsations is incorporated well. Rehme described the scattering of data to be due to geometrical tolerances of the test sections, the measuring techniques, and due to disturbances of the flow fields caused by probes and spacers.

3. ANALYSIS OF EXISTING DATA

There are several methods for evaluating the turbulent mixing flow rate. A number of researchers have calculated the turbulent mixing coefficients from measured subchannel temperatures coupled with computer simulations. The chemical tracer method, hot-wire anemometry, and laser Doppler anemometry are other possible experimental techniques. However, each of these methods has one or more limitations in terms of how they apply to rod bundle geometry, and considerable caution is required to obtain accurate data when using these methods. Therefore, the data for rod bundles is inadequate for developing a reliable correlation. Although several correlations have been developed for use in rod bundles, they show a rather large discrepancy relative to each other. This is mainly due to the scattering of the turbulent mixing data itself, which is used for the derivation of the correlations.

In Table 1, the experimental conditions for various turbulent mixing experiments are summarized. It is noted that most data for square rod arrays were obtained at a higher Reynolds number in a flow path with heated rods;

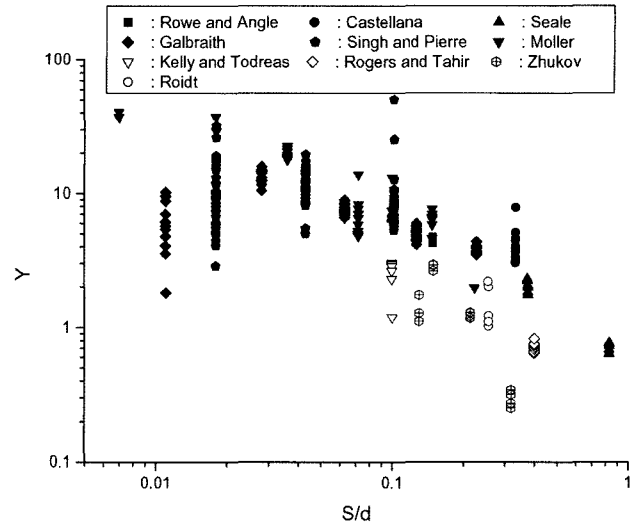


Fig. 2. Evaluated Turbulent Mixing Factor with the Definition of Y

therefore, the mixing factors were determined from the measured exit temperatures. In contrast, most data for triangular arrays were evaluated indirectly from the measured concentration of a tracer at a relatively low Reynolds number. The conditions for the experiments by Walton, Petrunik, and Kjellstrom in Table 1 were obtained from Ref. [12]. It should be noted that it requires considerable effort to obtain reliable mixing data with a tracer, as large entrance lengths are needed to obtain the asymptotic values of the mixing coefficients at low Reynolds numbers and high Prandtl numbers, as mentioned by Ramm [8]. Kelly and Todreas [12] also found that it was very difficult to remove the entrance effects and to exclude the effect of a diversion flow in experiments using tracers.

In Fig. 2, all of the experimental data of the turbulent mixing factor Y for the square rod arrays summarized in Table 1 is plotted against the gap-to-diameter ratio. In the figure, some data for triangular rod arrays is also shown. It is easily seen that the dependency of the mixing factor on the Reynolds number Re can not be excluded. The considerable scattering of the data could be due to the geometrical tolerances of the test sections, the measuring techniques, and the disturbances of the flow fields, as mentioned by Rehme [3].

By the way, the mixing factor, Y , defined by Eq. (5) does not include the effect of a turbulent Prandtl number for various coolants. The turbulent Prandtl number is defined by the ratio of the eddy diffusivity of momentum ϵ_M to the eddy diffusivity of energy ϵ_H . The turbulent Prandtl number for a liquid with a low Prandtl number, such as liquid metal, deviates considerably from those for air and/or water, as summarized in the paper by Kays [13]. Therefore, the turbulent mixing factor Y defined by Eq. (5) is appropri-

ate only for a fluid with a high Prandtl number when the turbulent Peclet number is also high, as described by Kays [13]. In other words, Eq. (5) well describes the heat transfer due to the turbulent mixing through a gap between rods when the relationship of $\epsilon_M/\epsilon_H = 1$ is valid and the heat

transfer can be described by

$$q_{ij} = \rho c_p \epsilon_M S_{ij} \left(\frac{\partial T}{\partial n} \right)_s = \rho c_p \epsilon_M S_{ij} \frac{T_i - T_j}{z_{ij,M}}, \quad (10)$$

Table 1. Summary of the Experimental Conditions of the Referenced Previous Studies

Experimenter	Channel Type	Fluid	Pr	d(mm)	S/d	Re	Experimental Technique	Heating Type simulated
Rowe and Angle (1964)	S-T	Water	1.0447	14.30	0.036 0.149	$4.2 \times 10^4 \sim 1.26 \times 10^5$ $6.0 \times 10^4 \sim 1.80 \times 10^5$	Exit enthalpy and code simulation	Electrical rod heating
Castellana (1974)	S-S	Water	0.82~0.93	10.72	0.334	$9.0 \times 10^4 \sim 4.90 \times 10^5$	Exit enthalpy and code simulation	Electrical rod heating
Seale (1979)	S-S	Air	0.702~0.709	50.00	0.100 0.375 0.833	$4.6 \times 10^4 \sim 9.10 \times 10^4$ $4.6 \times 10^4 \sim 1.90 \times 10^5$ $3.4 \times 10^4 \sim 3.00 \times 10^5$	Pitot-temperature probe for velocity and temperature distribution	Uniform duct wall heat flux
Singh and Pierre	S-S	Water and Air	Sc~1000 ~1	21.34 20.83 19.81	0.018 0.043 0.102	$1.3 \times 10^3 \sim 3.80 \times 10^4$	Tracer and mixing or Pressure balance	Plane source
Galbraith and Knudsen	S-S	Water	Sc~1000	25.40	0.011 0.028 0.063 0.127 0.228	$8.0 \times 10^3 \sim 3.00 \times 10^4$	Tracer and Pressure balance	Plane source
Moller	S-S	Air	0.7078	157.5 157.5 157.5 157.5 157.5 139.0	0.007 0.018 0.036 0.072 0.100 0.148 0.223	$\sim 5.0 \times 10^4$	Hot wire and microphone	-
Kelly and Todreas	T-T	Water	Sc~1000	38.10	0.100	$2.0 \times 10^3 \sim 2.4 \times 10^4$	Tracer and Pressure balance	Plane source
Walton	T-T	Water Air	Sc~1000	20.22	0.05 ~1	$1.9 \times 10^3 \sim 5.7 \times 10^3$ $4.8 \times 10^3 \sim 9.1 \times 10^4$	Tracer and Pressure balance	Plane source
Petrunik	T-T	Water Genetron	Sc~1000 3.5	19.81	0.033 0.068 0.13 0.13	$1.35 \times 10^3 \sim 1.08 \times 10^4$ $3.9 \times 10^3 \sim 2.5 \times 10^4$ $4.4 \times 10^3 \sim 3.8 \times 10^4$ $7.0 \times 10^3 \sim 4.5 \times 10^4$	Tracer and mixing balance Temp. measurement	Plane source
Rogers and Tahir (1975)	T-T	Air	~1	25.4	0.40	$8.1 \times 10^3 \sim 4.95 \times 10^4$	Tracer and Pressure balance	Plane source
Roidt	T-T	Air	~1	63.5	0.256	7.0×10^4	Tracer and Calculated Diversion cross plains	Point source
Kjellstrom	T-T	Air	~1	156.5	0.217	$1.5 \times 10^3 \sim 3.6 \times 10^5$	Hot wire anemometer	-
Zukov	T-T	Na NaK	0.0077 0.0237 0.0308 0.0300	14.0 12.0 24.7 15.8	0.150 0.130 0.214 0.320	$8.60 \times 10^3 \sim 3.70 \times 10^4$ $3.80 \times 10^3 \sim 1.70 \times 10^4$ $1.10 \times 10^4 \sim 4.10 \times 10^4$ $1.60 \times 10^4 \sim 5.00 \times 10^4$	Electro-magnetic device and micro-thermocouple	Central rod heating

where $z_{ij,M}$ represents the characteristic mixing length of the momentum between subchannels i and j . The eddy diffusivity of momentum ϵ_M is determined from the Reynolds stress parallel to the rod wall; thus, it is defined as

$$\epsilon_M = \frac{-\overline{u'w'}}{\partial u/\partial z}, \tag{11}$$

where u' is the fluctuating velocity in the axial direction and w' denotes the fluctuating velocity in the direction parallel to the walls, i.e., to the coordinate z at the gap between two rods.

The exact relationship of the heat transfer across the gap is described from the definition of ϵ_H , as follows:

$$q_{ij} = \rho c_p \epsilon_H S_{ij} \left(\frac{\partial T}{\partial n} \right)_S = \rho c_p \epsilon_H S_{ij} \frac{T_i - T_j}{z_{ij,H}}, \tag{12}$$

where $z_{ij,H}$ is the characteristic mixing length of the heat between subchannels i and j . The eddy diffusivity of energy ϵ_H parallel to the rod wall at the gap between two rods is defined as

$$\epsilon_H = \frac{\overline{w'T'}}{\partial T/\partial z}, \tag{13}$$

where T' is the temperature fluctuation. By comparing Eq. (12) to Eq. (5), the mixing factor, Y , is obtained, as described by

$$Y = \frac{\epsilon_H}{\epsilon_M} \cdot \frac{\delta_{ij}}{z_{ij,H}}. \tag{14}$$

If the experimental data is correlated with this definition of Y , it indicates that another source of data scattering is included, as the ratio of the effective eddy diffusivity of energy to the reference eddy viscosity changes significantly for different fluids and under different thermal-hydraulic conditions. Furthermore, the ratio of the effective mixing distance to the centroid distance is not conserved for different geometrical configurations, that is, for square arrays and for triangular arrays.

It is necessary to correlate all of the mixing data consistently, including the data for a fluid with a low Prandtl number, such as liquid metal, as the turbulent Prandtl number increases remarkably as the turbulent Peclet number decreases [13] although the data on this condition is scarce. For a treatment of the experimental mixing data, the mixing factor Y_H is suggested, as defined by

$$q_{ij} = \rho c_p \bar{\epsilon}_H S_{ij} Y_H \frac{T_i - T_j}{\delta_{ij}}, \tag{15}$$

where $\bar{\epsilon}_M$ is the reference eddy diffusivity of energy obtained in a circular tube.

At this point, by comparing Eq. (15) to Eq. (6), the result is

$$Y_H = \frac{w_{eff} \delta_{ij}}{\bar{\epsilon}_H}. \tag{16}$$

In addition, a comparison between Eqs. (12) and (15) yields

$$Y_H = \frac{\epsilon_H}{\bar{\epsilon}_H} \cdot \frac{\delta_{ij}}{z_{ij,H}} = Y \cdot Pr_t, \tag{17}$$

where Pr_t is the turbulent Prandtl number defined as $\bar{\epsilon}_M/\bar{\epsilon}_H$. The turbulent Prandtl number can be evaluated with the following correlation suggested by Kays [13]:

$$Pr_t = \frac{0.7}{Pe_t} + 0.85, \tag{18}$$

where Pe_t is the turbulent Peclet Number defined by $(\epsilon_M/\nu) Pr$. Pr is the Prandtl number and ν denotes the kinematic viscosity.

Eq. (17) implies that the geometry of a flow path is also a dominant parameter to determine turbulent mixing in rod bundles when the mixing is evaluated with the mixing factors Y or Y_H . In particular, the data for the square arrays and for the triangular arrays should be treated separately because the characteristic mixing length is usually different in the two configurations. It is notable that the transition from a laminar to a turbulent flow in the gap region occurs at different Reynolds numbers for square arrays and for

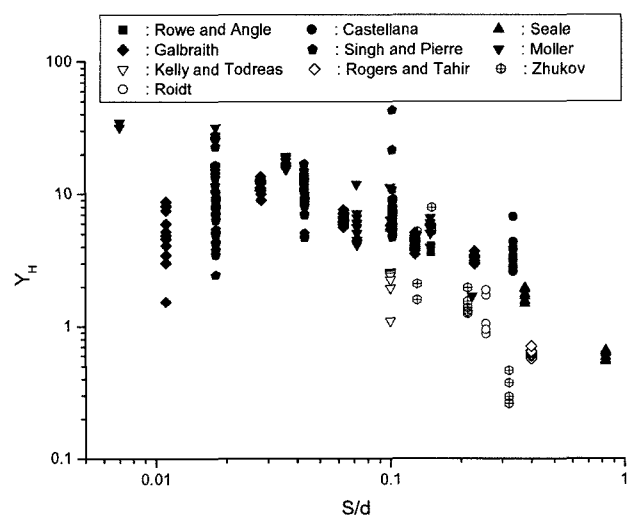


Fig. 3. Turbulent Mixing Data with the Definition of Y_H

triangular arrays at the same pitch-to-diameter ratio, as discussed by Ramm [8]. In Fig. 3, the data for the new mixing factor Y_H for various experiments is summarized. It is notable that the liquid metal data from Zhukov [14] show a change in Fig. 3 when compared with Fig. 2, as the turbulent Prandtl numbers of the liquid metals used by Zhukov are moderately different from those used in the other experiments.

4. DEVELOPMENT OF A CORRELATION

Combining the Eqs. (2), (4), (7) and (16), a useful relationship of the turbulent mixing factor is yielded, as follows:

$$Y_H = \left(\frac{\delta_{ij}}{D_h} \right) \cdot \left(\frac{\nu}{\bar{\epsilon}_H} \right) \cdot \text{Re} \cdot \beta, \tag{19}$$

or

$$Y_H = \left(\frac{\delta_{ij}}{D_h} \right) \cdot \left(\frac{\bar{\epsilon}_M}{\nu} \right)^{-1} \cdot \text{Re} \cdot \beta \cdot \text{Pr}_t. \tag{20}$$

In the above equations, D_h is the hydraulic diameter of a subchannel. If general expressions for the eddy diffusivity and the turbulent mixing coefficient β exist, it is possible to obtain a simple relationship for the turbulent mixing factor Y_H . In the present study, the aim is to develop a correlation

Table 2. Summary of the Major Parameters for the Mixing Factor Derived or Used by Researchers

Experimen-ter	S/d	Friction factor	Eddy diffusivity	w'_{ij}/μ	St_ξ or β	Y_H
Rowe and Angle (1964)	0.036 0.149	$f = a \cdot \text{Re}^b$	$\epsilon_H = 0.062 \cdot \text{Re}^{0.9}$	-	$0.063 \cdot \text{Re}^{-0.1}$ $0.021 \cdot \text{Re}^{-0.1}$	$\left(\frac{\delta_{ij}}{S} \right) \cdot \left(\frac{\bar{\epsilon}_M}{\nu} \right)^{-1} \text{Re} \cdot \beta \cdot \text{Pr}_t$
Castellana (1974)	0.334	$f = a \cdot \text{Re}^b$	$\epsilon_H/\nu \propto \text{Re} \sqrt{f/8}$	-	$0.027 \cdot \text{Re}^{-0.1}$	$\left(\frac{\delta_{ij}}{S} \right) \cdot \left(\frac{\bar{\epsilon}_M}{\nu} \right)^{-1} \text{Re} \cdot \beta \cdot \text{Pr}_t$
Seale (1979)	0.100 0.375 0.833	$f' = 0.053 \cdot \text{Re}^{-0.211}$ [Hussain & Reynolds]	$\epsilon_M/\nu = 0.00755 \cdot \text{Re}^{0.911}$	-	$0.02968 \cdot \text{Re}^{-0.1}$ $0.01683 \cdot \text{Re}^{-0.1}$ $0.009225 \cdot \text{Re}^{-0.1}$	$\left(\frac{\delta_{ij}}{S} \right) \cdot \left(\frac{\bar{\epsilon}_M}{\nu} \right)^{-1} \text{Re} \cdot \beta \cdot \text{Pr}_t$
Rogers and Roshart	-	-	-	-	$0.004 \cdot \left(\frac{D_h}{S} \right) \text{Re}^{-0.1}$	$\left(\frac{\delta_{ij}}{S} \right) \cdot \left(\frac{\bar{\epsilon}_M}{\nu} \right)^{-1} \text{Re} \cdot \beta \cdot \text{Pr}_t$
Rogers and Tahir (1975)	- 0.400	- $f' = 0.044 \cdot \text{Re}^{-0.194}$	-	$0.0050 \cdot \left(\frac{S}{d} \right)^{0.106} \text{Re}^{0.9}$ $0.0018 \cdot \left(\frac{S}{d} \right)^{-0.4} \text{Re}^{0.9}$	$\left(\frac{w'}{\mu} \right) \cdot \left(\frac{D_h}{S} \right) \text{Re}^{-0.1}$	$\left(\frac{\delta_{ij}}{S} \right) \cdot \left(\frac{\bar{\epsilon}_M}{\nu} \right)^{-1} \cdot \left(\frac{w'_{ij}}{\mu} \right) \cdot \text{Pr}_t$
Galbraith and Knudsen	0.011 0.028 0.063 0.127 0.228	-	-	$7.5 \times 10^{-15} \cdot \text{Re}^{3.43}$ $0.0001 \cdot \text{Re}^{1.23}$ $0.00037 \cdot \text{Re}^{1.12}$ $0.00050 \cdot \text{Re}^{1.12}$ $0.00190 \cdot \text{Re}^{1.01}$	$\left(\frac{w'}{\mu} \right) \cdot \left(\frac{D_h}{S} \right) \text{Re}^{-1}$	$\left(\frac{\delta_{ij}}{S} \right) \cdot \left(\frac{\bar{\epsilon}_M}{\nu} \right)^{-1} \cdot \left(\frac{w'_{ij}}{\mu} \right) \cdot \text{Pr}_t$
Kelly and Todreas (1977)	0.100	$f' = 0.0780 \cdot \text{Re}^{-0.288}$ [cf. Blasius eq.]	$\epsilon_H/\nu = 0.0045 \cdot \text{Re}^{0.89}$	$0.0021 \cdot \text{Re}^{0.935}$ [8000 < Re < 24000]	$\left(\frac{w'}{\mu} \right) \cdot \left(\frac{D_h}{S} \right) \text{Re}^{-1}$	$\left(\frac{\delta_{ij}}{S} \right) \cdot \left(\frac{\bar{\epsilon}_M}{\nu} \right)^{-1} \cdot \left(\frac{w'_{ij}}{\mu} \right) \cdot \text{Pr}_t$
Rehme	-	$f = 0.18 \cdot \text{Re}^{-0.2}$	$\bar{\epsilon}_M/\nu = 0.0075 \cdot \text{Re}^{0.9}$	-	-	-

of a turbulent mixing for a highly turbulent condition in square rod arrays.

4.1 Eddy Diffusivity

It is generally known that the eddy diffusivity is described with a Reynolds number and a friction factor, as follows:

$$\varepsilon \propto \nu \cdot \text{Re} \sqrt{f/8}, \quad (21)$$

where f is the Darcy friction factor. The friction factor is known to be a function of Reynolds number as follows:

$$f = a \cdot \text{Re}^b. \quad (22)$$

Therefore, the eddy diffusivity can be expressed as

$$\frac{\varepsilon}{\nu} = m \cdot \text{Re}^n. \quad (23)$$

Table 2 summarizes the expressions of the eddy diffusivity as suggested by several researchers. From the expression of the eddy diffusivity summarized in Table 2, it was found that the exponent n in Eq. (23) for the eddy diffusivity both in a circular tube and in rod arrays is approximately 0.9. Therefore, the eddy viscosity and kinematic viscosity have the following relationship in a highly turbulent region:

$$\frac{\bar{\varepsilon}_M}{\nu} = K \cdot \text{Re}^{0.9}, \quad (24)$$

which can be used as a reference eddy viscosity to evaluate the turbulent mixing factor Y_H with Eq. (20).

Kays [15] proposed an empirical equation for a friction factor in a circular tube applicable over the range $3 \times 10^4 < \text{Re} < 10^6$, as follows:

$$f = 0.184 \cdot \text{Re}^{-0.2}. \quad (25)$$

Table 3. Summary of the Experimental Results for the Turbulent Mixing Factor

Experimenter	Channel Type/Fluid	S/d	D _h (mm)	δ _y /D _h	St _g or β	A	Pr _t	Y*	Y _H *
Rowe and Angle (1964)	S-T/Water	0.036	5.105	2.488	0.063 · Re ^{-0.1}	0.063	0.853	20.675	17.636
		0.149	7.290	1.769	0.021 · Re ^{-0.1}	0.021	0.853	4.901	4.180
Castellana (1974)	S-S/Water	0.334	13.56	1.054	0.027 · Re ^{-0.1}	0.027	0.851	3.754	3.195
Seale (1979)	S-S/Air	0.100	27.1	1.7176	0.02968 · Re ^{-0.1}	0.02968	0.856	6.725	5.757
		0.375	57.3	0.9296	0.01683 · Re ^{-0.1}	0.01683	0.855	2.064	1.765
		0.833	125.0	0.5710	0.009225 · Re ^{-0.1}	0.009225	0.855	0.695	0.591
Rogers and Roshart (1972)	S-S	-	-	-	0.004 $\left(\frac{D_h}{S}\right) \text{Re}^{-0.1}$	-	-	-	-
Galbraith and Knudsen	S-S	0.011	10.57	2.6442	2.8365x10 ⁻¹³ · Re ^{2.43}	-	-	-	-
		0.028	11.17	2.5011	0.001571 · Re ^{0.23}	-	-	-	-
		0.063	12.42	2.2504	0.002871 · Re ^{0.12}	-	-	-	-
		0.127	14.69	1.9018	0.00227 · Re ^{0.12}	-	-	-	-
		0.228	18.29	1.5280	0.005999 · Re ^{0.01}	-	-	-	-
Rogers and Tahir (1975)	S-S	-	-	-	0.005 · $\left(\frac{D_h}{S}\right) \cdot \left(\frac{S}{d}\right)^{0.106} \cdot \text{Re}^{-0.1}$	-	-	-	-
	T-T/Air	0.400	29.4	0.699	0.007479 · Re ^{-0.1}	0.007479	0.866	0.644 ~0.829	0.565 ~0.709
Kelly and Todreas (1977)	T-T/Water	0.100	12.733	1.9000	0.0070 · Re ^{-0.065}	-	0.850	1.196 ~3.042	1.107 ~2.586

As suggested by several researchers [3,10,11], it is possible to evaluate the reference eddy viscosity expressed by

$$\frac{\bar{\epsilon}_M}{\nu} = \frac{Re}{20} \sqrt{\frac{f}{8}} \quad (26)$$

Combining Eqs. (25) and (26) yields a reference eddy viscosity for $3 \times 10^4 < Re < 10^6$, given by

$$\frac{\bar{\epsilon}_M}{\nu} = 0.00758 \cdot Re^{0.9}, \quad (27)$$

which is nearly identical to the reference eddy viscosity used by Rehme [3].

4.2 Turbulent Mixing Stanton Number

All of the available experimentally-determined correlations on a turbulent mixing coefficient or a turbulent mixing Stanton number β are summarized in Tables 2 and 3. The same correlations are also compared with each other in Fig. 4. The data shows relatively scattered characteristics, as the geometry and the range of the Reynolds number for each experiment differ greatly. Essentially, this was the main reason for the difficulty that many previous researchers encountered while trying to obtain a generalized correlation for turbulent mixing factors. Therefore, the applicable range of most existing correlations is limited to a certain range of the Reynolds number and to the specified geometries.

Fig. 4 indicates clearly that the turbulent mixing decreases as the gap-to-diameter ratio S/d increases. Furthermore, it was found that turbulent mixing is generally reduced with an increase in the Reynolds number despite the fact that the effect of the Reynolds number diminishes as it becomes higher, especially with a large gap-to-diameter ratio. However, this trend is not inconsequential at a lower Reynolds number. In the figure, the turbulent mixing Stanton number obtained by Kelly and Todreas [12] in triangular rod arrays decreases as the Reynolds number decreases to lower than 8,000 where the effect of a laminarization appears. The results by Galbraith and Knudsen [16] also show the laminarization effect as the Reynolds number decreases in square rod arrays. Therefore, the data obtained at a lower or intermediate range of a Reynolds number is not applicable to the development of a correlation for a highly turbulent condition.

The experiments by Rowe and Angle [4], Castellana [5], and Seale [6] were performed at Reynolds numbers higher than 3.0×10^4 using the exit temperature or enthalpy measurement in square rod arrays. In these experiments, the error for the turbulent mixing rate induced by the measurement technique itself is much less than the experiment using a tracer technique. The major error with this type of experiment would come from the entrance effect if the length of the test section is insufficient. Although there

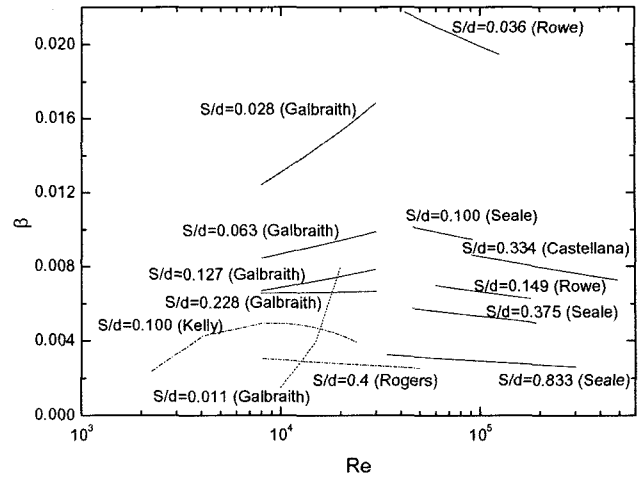


Fig. 4. Various Experimental Results for the Mixing Stanton Number

exists a considerable scattering for the turbulent mixing coefficient, all of the experimenters who measured the mixing coefficients at Reynolds numbers higher than 3.0×10^4 commonly summarized their experimental data into the form of

$$\beta = A \cdot Re^{-0.1} \quad (28)$$

The value of A varies depending on the test section geometry, as summarized in Table 3 and also depicted in Fig. 4.

4.3 Turbulent Mixing Correlation for a Highly Turbulent Condition

With the previously determined eddy diffusivity of Eq. (27) and the turbulent mixing Stanton number of Eq. (28), Eq. (20) is converted to

$$Y_H = \frac{A}{K} \cdot \left(\frac{\delta_{ij}}{D_h} \right) \cdot Pr_r \quad (29)$$

The above equation implies that the turbulent mixing factor is nearly independent of the Reynolds number and that the geometrical factors are the most important parameters affecting the turbulent mixing under a highly turbulent condition. The final forms of the turbulent mixing factor can be obtained with two different methods.

The first approach is to have an expression of $(A \cdot Pr_r)$ dependent on the geometrical factors to obtain a simple relationship of the turbulent mixing factor. Fortunately, this expression can be derived from the experimental results. Although the amount of data is very limited, the experi-

mental data by Rowe and Angle, Castellana, and Seale are roughly correlated as

$$A \cdot Pr_t \approx 0.01996 \cdot \left(\frac{\delta_{ij}}{D_h} \right). \quad (30)$$

Therefore, the turbulent mixing factor is expressed roughly by the following relationship:

$$Y_H \approx 2.633 \cdot \left(\frac{\delta_{ij}}{D_h} \right)^2. \quad (31)$$

The second method is to obtain a correlation in the form of Eq. (29) through a direct evaluation of the experimental data for a turbulent mixing. The data provided by Rowe and Angle, Castellana, and Seale is used for the evaluation. All of the non-dimensional turbulent mixing factors are correlated into the following form, as shown in Fig. 5:

$$Y_H = 2.037 \cdot \left(\frac{\delta_{ij}}{D_h} \right)^{2.071}. \quad (32)$$

In Fig. 6, the same data is correlated with the variable S/d into the following expression:

$$Y = 0.7709 \cdot \left(\frac{S_{ij}}{d} \right)^{-0.9978}, \quad (33)$$

which is very similar to Rehme's correlation [3], as shown in the figure. Therefore, the applicability of the correlation developed by Rehme is evaluated as limited to the highly turbulent condition in square rod arrays although mixing

data, both for the square arrays and for the triangular arrays, has been used for the derivation of the correlation.

In Fig. 7, the developed turbulent mixing correlation of Eq. (32) is evaluated with the available mixing data. It is noted that the correlation predicts a reasonable mixing at a higher δ_{ij}/D_h , i.e., a lower S/d ratio in which most existing correlations overestimate the mixing rate. It should be noted that the derived correlation is applicable in the range of

$$3.0 \times 10^4 \leq Re \leq 1.0 \times 10^6,$$

and

$$0.57 \leq \frac{\delta_{ij}}{D_h} \leq 2.94.$$

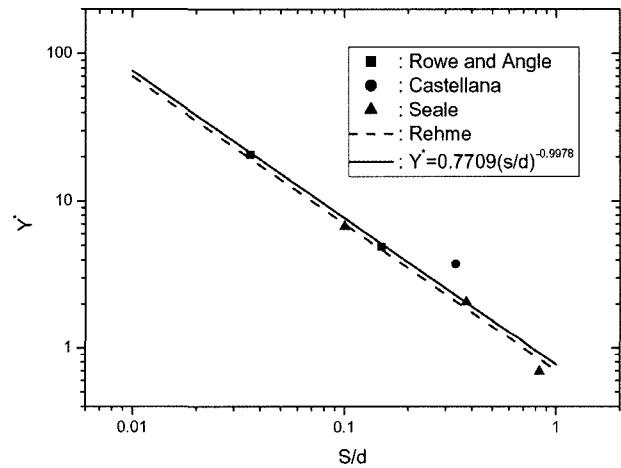


Fig. 6. Comparison of the Re-independent Mixing Data with Rehme's Correlation

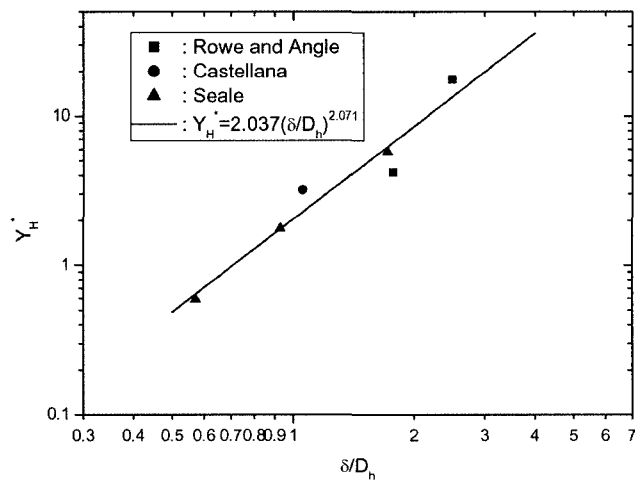


Fig. 5. Re-independent Turbulent Mixing Factor for Square Arrays

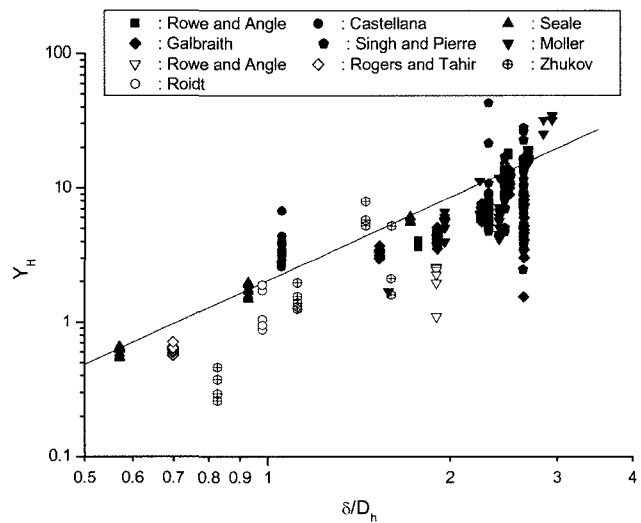


Fig. 7. Evaluation of the Developed Correlation with the Turbulent Mixing Data

5. CONCLUSIONS

To take into account a turbulent mixing for fluids with various Prandtl numbers, a new definition of a turbulent mixing factor is introduced. With this definition of a mixing factor, it was found that the geometrical parameter, δ_{ij}/D_h , correlates the turbulent mixing data better than S/d , which is used frequently in existing correlations. Based on the experimental data for a highly turbulent condition in square rod arrays, the useful correlation shown in Eq. (32) was developed. This correlation shows that the dependency of the turbulent mixing factor on Re is negligible under highly turbulent conditions, and it predicts reasonable mixing at a higher δ_{ij}/D_h or at a lower S/d ratio, which is the feature of the correlation that is most improved when compared with existing correlations. The applicability of the proposed correlation to triangular arrays should be investigated with more experimental data for a triangular array and for a low Prandtl number fluid as well.

ACKNOWLEDGEMENT

This work was performed under the Long-term Nuclear R & D Program supported by the Ministry of Science and Technology (MOST), Korea.

REFERENCES

- [1] H. Y. Jeong, K. S. Ha, W. P. Chang, Y. M. Kwon and Y. B. Lee, "Modeling of Flow Blockage in a Liquid Metal-Cooled Reactor Subassembly with a Subchannel Analysis Code," *Nuclear Technol.*, **149**, 71 (2005).
- [2] C. W. Stewart, C. L. Wheeler, R. J. Cena, C. A. McMonagle, J. M. Cuta and D. S. Trent, "COBRA-IV: The model and the method," BNWL-2214, Pacific Northwest Laboratories (1977).
- [3] K. Rehme, "The Structure of Turbulence in Rod Bundles and the Implications on Natural Mixing between the Subchannels," *Int. J. Heat Mass Transfer*, **35**, 567 (1992).
- [4] D. S. Rowe and C. W. Angle, "Crossflow Mixing between Parallel Flow Channels during Boiling, Part II: Measurement of Flow and Enthalpy in Two Parallel Channels," BNWL-371 PT2, Pacific Northwest Laboratory (1967).
- [5] F. S. Castellana, W. T. Adams, and J. E. Casterline, "Single-Phase Subchannel Mixing in a Simulated Nuclear Fuel Assembly," *Nucl. Eng. Des.*, **26**, 242 (1974).
- [6] W. J. Seale, "Turbulent Diffusion of Heat between Connected Flow Passages, Part I: Outline of Problem and Experimental Investigation," *Nucl. Eng. Des.*, **54**, 183 (1979).
- [7] S.-K. Cheng and N. F. Todreas, "Constitutive Correlations for Wire-Wrapped Subchannel Analysis under Forced and Mixed Convection Conditions," DOE/ET/37240-108TR, MIT, Cambridge, Massachusetts (1984).
- [8] H. Ramm, K. Johannsen and N. E. Todreas, "Single Phase Transport within Bare Rod Arrays at Laminar, Transition and Turbulent Flow Conditions," *Nucl. Eng. Des.*, **30**, 186 (1974).
- [9] J. T. Rogers and A. E. E. Tahir, "Turbulent Interchange Mixing in Rod Bundles and the Role of Secondary Flows," ASME Paper 75-HT-31 (1975).
- [10] L. Ingesson and S. Hedberg, "Heat Transfer between Subchannels in a Rod Bundle," *Heat Transfer 1970*, Paris, Vol. **III**, FC 7.11, Elsevier, Amsterdam (1970).
- [11] S. V. Moller, "Single-Phase Turbulent Mixing in Rod Bundles," *Exp. Thermal Fluid Sci.*, **5**, 26 (1992).
- [12] J. M. Kelly and N. E. Todreas, "Turbulent Interchange in Triangular Array Bare Rod Bundles," COO-2245-45TR, MIT, Cambridge, Massachusetts (1977).
- [13] W. M. Kays, "Turbulent Prandtl Number-Where Are We?," *J. Heat Transfer*, **116**, 284 (1994).
- [14] A. V. Zhukov, N. A. Kotovskii, L. K. Kudryavtseva, N. M. Matyukhin, E. Ya. Sviridenko, A. P. Sorokin, P. A. Ushakov and Yu. S. Yur'ev, "Comecon-Symposium "Teplofizika i gidrodinamika aktivnoi zony i parogeneratorov dlya bystrykh reaktorov," Marianske Lazne, CSSR, April 4-8, 1978, CKAE, Prag 1978, Vol. 1, Paper ML 78/09, 114-127 (in Russian); German translation KfK-tr-657, Kernforschungszentrum Karlsruhe, F.R.G. (1980).
- [15] W. M. Kays and H. C. Perkins, "Forced Convection, Internal Flow in Ducts," *Handbook of Heat Transfer Fundamentals*, **2nd ed.**, p. 7-5, McGraw-Hill, Inc. (1985).
- [16] K. P. Galbraith and J. G. Knudsen, "Turbulent Mixing between Adjacent Channels for Single-Phase Flow in a Simulated Rod Bundle," 12th Natn. Heat Transfer Conf., Tulsa, Oklahoma, *AIChE Symposium Series*, No. 118, Vol. 68, pp.90-100 (1971).
- [17] K. Singh and C. C. St. Pierre, "Single Phase Turbulent Mixing in Simulated Rod Bundle Geometries," *Trans. CSME*, **1**(2), 73 (1972).
- [18] M. Roidt, M. J. Pechersky, R. A. Markley and B. J. Vegter, "Determination of Turbulent Exchange Coefficients in a Rod Bundle," *J. Heat Transfer*, 172-177 (1974).
- [19] J. T. Rogers and R. G. Rosehart, "Mixing by Turbulent Interchange in Fuel Bundles. Correlations and Influences," ASME Paper 72-HT-53, *AIChE-ASME Heat Transfer Conference*, Denver, Colorado, August 6-9, 1972.